Extreme Mechanics Letters 39 (2020) 100803

Contents lists available at ScienceDirect

Extreme Mechanics Letters

journal homepage: www.elsevier.com/locate/eml

Topological adhesion. I. Rapid and strong topohesives

Jason Steck, Junsoo Kim, Jiawei Yang, Sammy Hassan, Zhigang Suo *

John A. Paulson School of Engineering and Applied Science, Kavli Institute for Nanobio Science and Technology, Harvard University, Cambridge, MA 02138, USA

ARTICLE INFO

Article history:
Received 25 April 2020
Received in revised form 29 May 2020
Accepted 1 June 2020
Available online 6 June 2020

Keywords:
Adhesion
Hydrogel
Topological entanglement
Kinetics
Topohesion

ABSTRACT

Topological adhesion, or topohesion for brevity, links two polymer networks, to be called adherends, even when the adherend networks carry no functional groups for chemical coupling. Uncrosslinked polymers, called stitch polymers, are spread between the two adherends. In response to a trigger, the stitch polymers form a stitch network in topological entanglement with both adherend networks. It is commonly believed that topohesion always takes a long time, but this is a misconceived myth. In principle, two adherends topohere strongly even when the stitch network entangles with each adherend network by a single polymer mesh size. The shallowness of this requirement dictates that topohesion is rate-limited by the gelation of the stitch network, not by the diffusion of the stitch polymers into the adherend networks. We illustrate this concept using two pieces of polyacrylamide hydrogels as adherends, an aqueous solution of cellulose as stitch polymers, and a change in the pH in the cellulose solution as a trigger. By varying the thickness of the cellulose solution, the time to topohere is tunable from seconds to hours. For a solution of thickness of 50 microns adhesion energy of 50 Jm^{-2} is attained in 60 s. These experimental findings dispel the myth, and shed light on the times to topohere reported in the literature. The art and science of topohesion provide fertile grounds for fundamental discovery and practical invention to enable unusual applications.

1. Introduction

A soft biological tissue often consists of water molecules and a polymer network. This molecular architecture enables two basic functions: wetness and elasticity. The water molecules provide liquid-like wetness to enable molecules and ions to react and migrate, while the polymer network provides solid-like elasticity to enable large and reversible deformation. Since the 1960s, this molecular architecture has been mimicked by synthetic hydrogels [1,2]. The integration of wet and elastic materials – biological and synthetic – underpins many technologies of our time. Examples include tissue repair [3–7], wound closure [8–11], drug delivery [12–15], bioelectronics [16–19], and wearable devices [20–28].

The integration of diverse wet and elastic materials poses a fundamental challenge: create strong adhesion that preserves the dual functions of wetness and elasticity. First, water molecules at the interface must maintain liquid-like wetness, so that mobile molecules can transmit freely from one material to the other. Second, the polymer networks of the two materials must fuse and retain solid-like elasticity, so that the integrated materials as a whole can undergo large and reversible deformation. The adhesion is called strong if the adhered materials can sustain deformation comparable to that of individual adherends. The liquid-like water molecules readily change neighbors, and contribute negligibly to strong adhesion [23]. A wet, elastic, strong adhesion links the adherend networks in two basic ways—bond and stitch [23,29]. In bond, the two polymer networks form interlinks, either with each other, or with some intermediate objects, such as inorganic particles [30] and polymers [5,31–34]. In stitch, the two polymer networks both topologically entangle with a third polymer network, called the stitch network [35–39]. Both ways of wet, elastic, strong adhesion ensure that the integrated materials preserve the dual functions: liquid-like wetness and solid-like elasticity. Adhesion by bond requires that the networks of both adherends carry functional groups for chemical coupling, whereas adhesion by stitch does not. Prior to the breakthrough in recent years, no wet, elastic, strong adhesion had been reported. For instance, cyanoacrylate forms a plastic, which blocks the permeation of water and other mobile species, and restrains deformation. Various protein-based adhesives are weak; they provide neither strong bonds nor topological entanglements. See a review on wet, elastic, strong adhesion [29].

Here we start a series of papers on the art and science of adhesion by stitch, also called topological adhesion, or topohesion for short. In topohesion, each of the two adherends has a polymer network, which need carry no functional groups for chemical coupling. Water-dissolvable polymers, called the stitch polymers, are

* Corresponding author.
E-mail address: suo@seas.harvard.edu (Z. Suo).

https://doi.org/10.1016/j.eml.2020.100803
2352-4316/

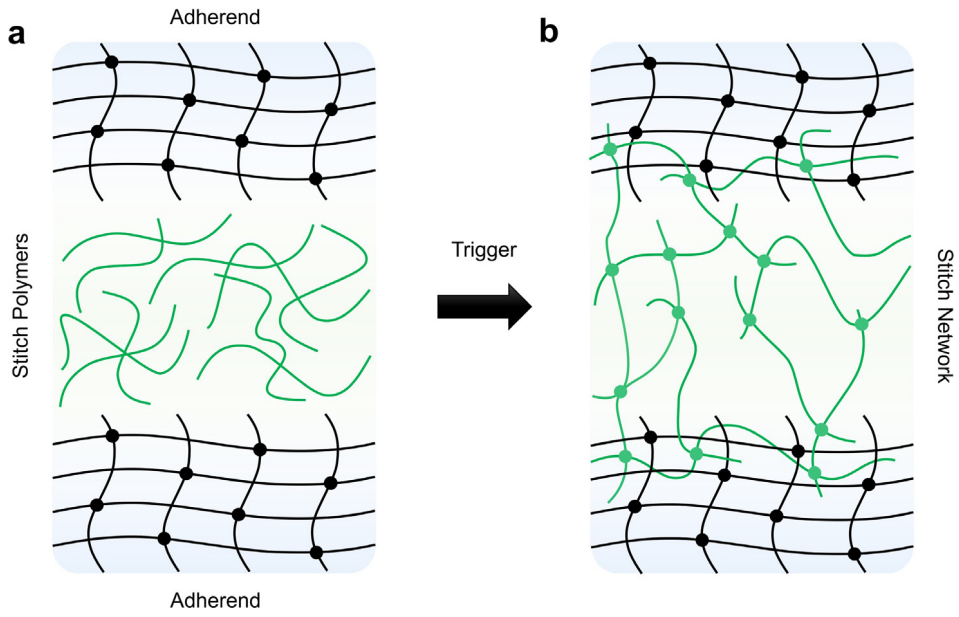

Fig. 1. Principle of topological adhesion. (a) Each adherend has a polymer network, but carries no functional group for chemical coupling. A solution of stitch polymers is spread between the two adherends. (b) In response to a trigger, the stitch polymers form a stitch network, in topological entanglement with the two adherend networks. In principle, strong adhesion is achieved even when the stitch network entangles with each adherend network by a single polymer mesh size.

spread between the two adherends, either as an aqueous solution, or as a dry powder (Fig. 1a). In response to a trigger, the stitch polymers form a stitch network, in topological entanglement with the two adherend networks (Fig. 1b). The three networks form no chemical bonds with one another, but their separation requires at least one network to rupture.

Strong topohesion can be superficial. This remarkable fact is of fundamental significance to topohesion, but has yet been appreciated. Assuming that the stitch network itself is strong, topohesion is strong, in principle, even when the stitch network entangles with a single polymer mesh size of each adherend network. This superficial requirement is understood as follows. An adherend has a sparse polymer network. To strongly adhere two such adherends by chemical bonds, the bonds just need to interlink the polymers on the surfaces of the two adherends, and the interlinks between the two adherends can be as sparse as the crosslinks within each adherend. Similarly, to strongly adhere two adherends by topological entanglement, the stitch network just needs to entangle with a single mesh size of each adherend network, and the stitch network can be as sparse as the adherend networks. Consequently, the stitch polymers need only penetrate one mesh size into each adherend before forming the stitch network.

The shallow requirement of the stitch network dictates that the time to topohere be governed by the gelation of the stitch network, not by the diffusion of the stitch polymers into the adherend networks. This picture dispels the misconception that topohesion must be slow. Strong topohesion can be attained rapidly, and the time to topohere is tunable. We demonstrate these facts using polyacrylamide hydrogels as adherends, an aqueous solution of cellulose as stitch polymers, and a change in the pH of the solution as the trigger. The time of gelation is governed by the time needed to change the pH in the topohesive, which requires the dilution of OH^- ions in the topohesive. By varying the thickness of the cellulose solution, we tune the time to adhere from seconds to hours. That topohesion can be rapid poses a question. Why are many reported methods of topohesion so slow, often taking hours? We discuss the kinetics of these methods of topohesion and propose ways to tune their times to topohere.

2. Cellulose topohesive

This paper demonstrates that topohesion can be rapid, and that the time to topohere is tunable. We do so by using cellulose to topohere two pieces of polyacrylamide (PAAm) hydrogel. PAAm hydrogel is a model adherend for wet, elastic, strong topohesion in that it has a covalent polymer network and carries no functional groups for chemical coupling. Cellulose is used in familiar commercial products such as paper, cellophane, and textile, and the chemistry of cellulose has been extensively studied [40,41]. Cellulose is a polysaccharide consisting of a linear chain of D-glucose units. When cellulose is in contact with water, the hydroxyl groups on cellulose undergo an acid–base reaction $XOH \rightleftarrows XO^- + H^+$, where X represents the backbone of the cellulose polymer. The equilibrium constant of this reaction is set by the quotient of the concentrations, $K_a = [XO^-][H^+]/[XOH]$. By definition, $pK_a = -\log K_a$ and $pH = -\log [H^+]$, so that $\log[XO^-] - \log[XOH] = pH - pK_a$. For cellulose, $pK_a = 13$. When pH > 13, more hydroxyl groups are deprotonated and carry negative charges, $[XO^-] > [XOH]$, and cellulose is a soluble polyelectrolyte (Fig. 2a). When pH < 13, more hydroxyl groups are protonated, $[XO^-] < [XOH]$, and cellulose chains crosslink into a polymer network by OH-OH hydrogen bonds (Fig. 2b). The cellulose topohesive has a low viscosity at the concentrations required for tough adhesion, and topoheres hydrogels of an enormous range of pH, any value below 13.

We topohere using a procedure described in a previous study [35]. We prepare two pieces of PAAm hydrogels at pH 7. We prepare an aqueous solution of cellulose, sodium hydroxide (NaOH), and urea at pH 14 [42]. NaOH fully dissociates into sodium and hydroxyl ions in water, and sets the high pH. Urea assists the dissolution of crystalline cellulose fibers into polymer chains. We spread this aqueous solution on the surface of one PAAm hydrogel and immediately press a second PAAm hydrogel on top (Fig. 2c). The cellulose polymer, Na^+, OH^-, and urea diffuse into the hydrogels concurrently. As OH^- dilutes, the pH of the interface drops, and the cellulose chains crosslink into a polymer network, in topological entanglement with both PAAm networks (Fig. 2d).

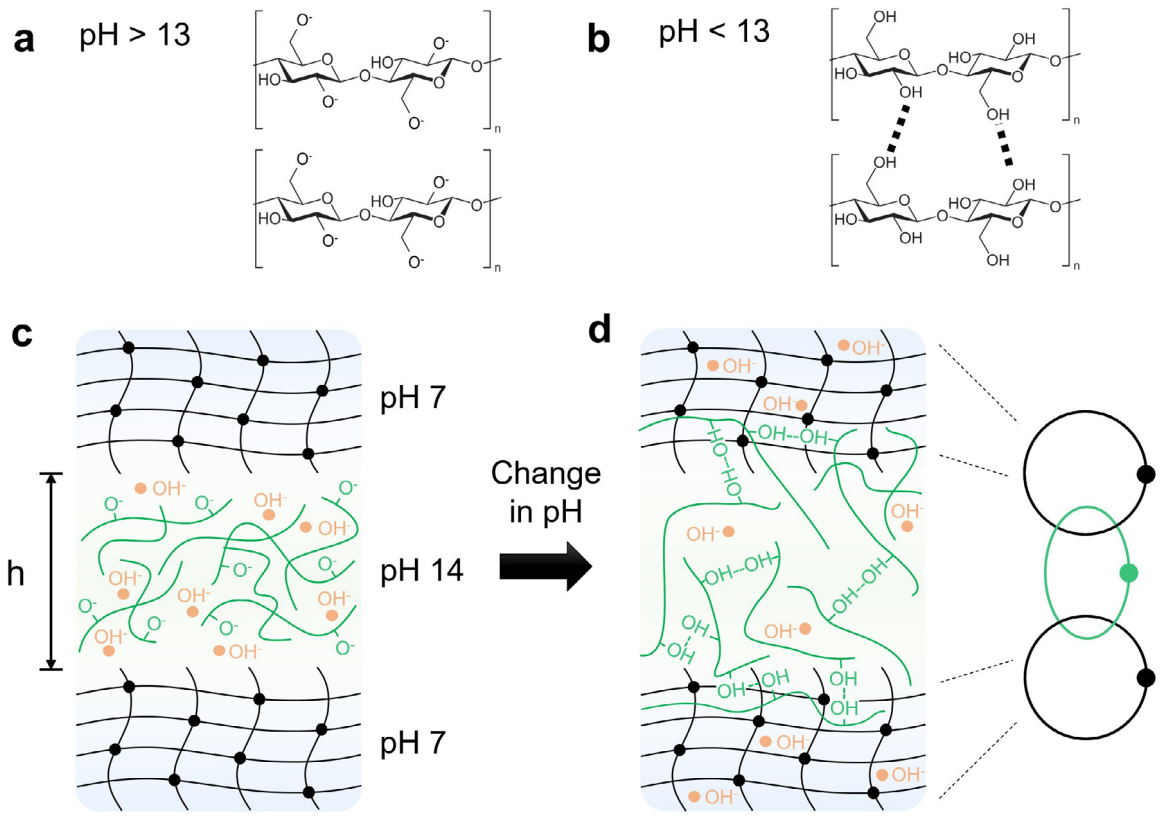

Fig. 2. Cellulose topohesive. (a) Cellulose forms a polymer solution in water at a high pH. (b) The polymers form a network through hydrogen bonds when the pH is reduced. (c) Two polyacrylamide hydrogels of pH = 7 act as adherends, and an aqueous solution of cellulose at pH = 14 acts as stitch polymers. The solution of cellulose, thickness h, is spread between the two hydrogels. (d) As the concentration of OH^- in the cellulose solution reduces, the cellulose polymers form a stitch network, in topological entanglement with the two polyacrylamide networks.

We apply light compression to squeeze out excess solution (Fig. 3a), and then let the gels adhere without any prolonged compression. We use 180-degree peel to measure adhesion energy (Fig. 3b). The two hydrogels are attached with inextensible backing layers. As the loading machine pulls the backing layers at a constant velocity, the crack advances at a velocity equal to one-half of the machine velocity. Once in steady-state peel, the adhesion energy is calculated as twice the steady-state force divided by the width of the sample. We measure adhesion energy 24 h after adhering to ensure that the sample has reached equilibrium. The adhesion energy increases with the concentration of cellulose, reaching an adhesion energy of ∼200 J m^{-2} at a cellulose concentration of 2 wt% (Fig. 3c). This adhesion is strong, as the adhesion energy is comparable to the fracture energy of the PAAm hydrogel. By contrast, directly attaching two pieces of PAAM hydrogel without the cellulose solution produces a low adhesion energy of ∼10 J m^{-2}. Cellulose solution of a concentration of 2 wt% is used in all subsequent experiments. Adhesion energy increases with time after contact (Fig. 3d). An appreciable adhesion energy of 10 J m^{-2} is observed 100 s after bonding, which is similar to the adhesion energy between two bare PAAm hydrogels. The adhesion energy increases after this time, reaching a value of 50 J m^{-2} in 170 s.

3. Tunable time to topohere

Gelation of the cellulose solution is triggered by a drop of pH—that is, the dilution of OH^- ions in the solution. We assume the acid–base equilibrium of water, $[OH^-][H^+] = 10^{-14}$, and the acid–base equilibrium of cellulose, $[XO^-][H^+]/[XOH] = 10^{-13}$. The initial cellulose solution is highly basic, $[OH^-] > 10^{-1}$ M. To dilute OH^- ions in the cellulose solution, OH^- ions may migrate from the cellulose solution into the adherends, and water molecules may migrate from the adherends into the cellulose solution. Thus, the dilution of OH^- ions in the cellulose solution involves multiple reactions and multiple mobile species. The coupled reaction–diffusion process is complicated to study quantitatively in detail. Nevertheless, the initial thickness of the cellulose solution, h, sets the length scale for diffusion. The time for the cellulose to gel is set by the migration of these mobile species across this length, and is expected to scale as $t \sim h^2/D_{\text{trigger}}$, where D_{trigger} is an effective diffusivity. This scaling relation implies that the time to adhere can be tuned by modifying the thickness of the topohesive solution. A two-fold reduction in thickness results in a four-fold reduction in the time to adhere.

To test this idea quantitatively, we use a nylon mesh as a spacer to control the initial thickness of the cellulose solution (Fig. 4a). We immerse the nylon mesh into the 2 wt% cellulose solution and wipe away any excess solution so that the thickness of the applied solution scales with the thickness of the dry nylon mesh. The wetted mesh is then placed between two PAAm hydrogels. Only the compression required to ensure wetted contact is applied to the adhered gels. We then measure the adhesion energy as a function of time after contact (Fig. 4b). Four different thicknesses were tested, including meshes with thicknesses of 50, 120, and 180 μm, as well as the thickness achieved by applying free cellulose solution onto the gels and compressing (Fig. 3a). For the 50-μm film, the adhesion energy reaches 50 J m^{-2} in ∼60 s, and equilibrium in ∼10 min. For the 120-μm film, the adhesion energy reaches 50 J m^{-2} in ∼250 s, and equilibrium in ∼20 min. By increasing the thickness to 180 μm, the time for the adhesion energy to develop to 50 J m^{-2} is increased to ∼500 s. The adhesion energy data for the compressed topohesive

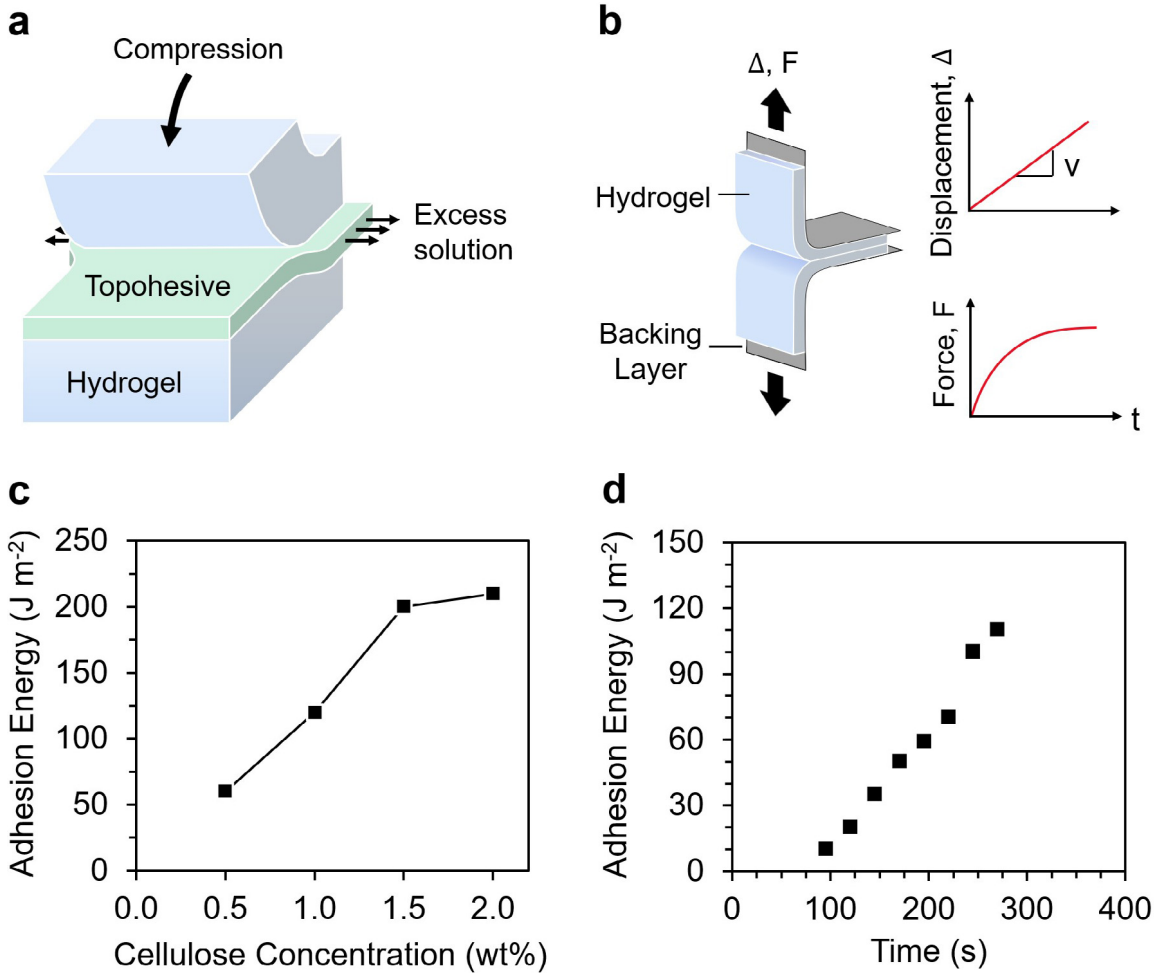

Fig. 3. Adhesion energy. (a) Adhesion is formed by spreading cellulose polymer solution between two hydrogels, and subsequently applying compression to remove excess solution. Compression is removed after contact. (b) 180-degree peel. A loading machine pulls the backing layers, and records the peel force. Adhesion energy is calculated as the twice the steady-state peel force divided by the width of the sample. (c) Adhesion energy as a function of cellulose concentration, measured at 24 h after contact. (d) Adhesion energy increases with time after contact; the initial solution contains 2 wt% of cellulose.

is plotted alongside the data for the nylon meshes (Fig. 4b). The compressed cellulose data lies between that of the 50-μm and 120-μm films.

We now test the scaling relation proposed for pH-triggered topohesion, $t \sim h^2/D_{\text{trigger}}$. Like any kinetic process, topohesion approaches equilibrium asymptotically. Consequently, the time to achieve equilibrium adhesion is poorly defined. Instead, we quantify the time to adhere by the time when the adhesion energy reaches half of its equilibrium value. For cellulose, the equilibrium adhesion energy is taken to be 200 J m^{-2} for all thicknesses, and the time to reach 100 J m^{-2} is defined as the time at half of the maximum adhesion energy. The time at half max is then plotted as a function of the thickness (Fig. 4c). When plotted logarithmically, the time at half max is linear in the thickness with a slope of 2. This observation is in agreement with the scaling relation $t \sim h^2$. We then revisit the data for pH-triggered topohesion using a chitosan stitch polymer [35]. A chitosan topohesive reaches an equilibrium adhesion energy of 150 J m^{-2}. Therefore, half of the equilibrium adhesion energy is 75 J m^{-2} and the time at half max is ∼5 h. The thickness is controlled to be 500 μm. Even though the chemistry of the stitch polymer is different between the two topohesives, the adhesion time of the chitosan topohesive lies along the thickness-squared relation set by the cellulose topohesive. This suggests that, for pH-triggered topohesion, the particular chemistry of the stitch polymer does not significantly affect the time to adhere. However, it should be noted that additional variables could alter the time to adhere that have not yet been studied, such as the presence of a buffer, the pH of the hydrogel, and the pH of the topohesive. These variables would need to be tested to confirm the validity of this relation in pH-triggered topohesives of disparate chemistries. Assuming the scaling relation $t \sim h^2/D_{\text{trigger}}$, the intercept of the line in Fig. 4c estimates the effective diffusivity, $D_{\text{trigger}} = 2.35 \times 10^{-11}$ m^2 s^{-1}. This value is smaller than the diffusivities of ions in water typically reported, which are on the order of 10^{-9} m^2 s^{-1}. The discrepancy may be due to the unknown numerical coefficient in the scaling relation. This numerical coefficient may originate from details regarding the coupled reaction–diffusion process and the diffusivity of solutes in the crosslinked polymer network.

A 500-μm thick adhesive results in an adhesion time on the order of hours, while a 50-μm thick adhesive results in an adhesion time on the order of minutes. The scaling relation $t \sim h^2$ suggests that topological adhesion can be made even faster by reducing the thickness further. In principle, the lower limit of this relation is the time required for the stitch network to entangle with each adherend network by a single mesh size. We take the diffusivity of the stitch polymer D_{stitch} to be 10^{-12} m^2 s^{-1} and the mesh size of the adherend network L_{mesh} to be 10^{-8} m. The time scale for diffusion of stitch polymer is then estimated by $t \sim L^2_{\text{mesh}}/D_{\text{stitch}}$ to be on the order of 10^{-4} s. Taking the effective diffusivity of the trigger D_{trigger} to be 10^{-11} m^2 s^{-1}, the thickness

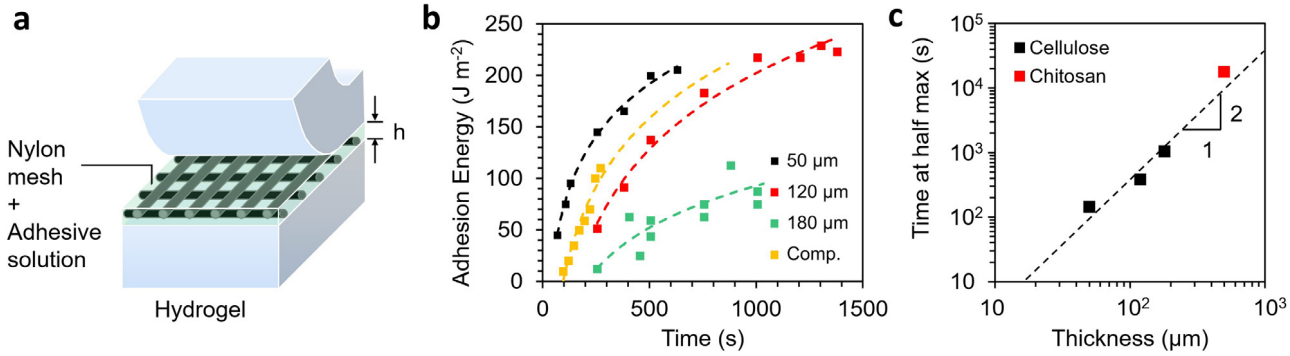

Fig. 4. Tunable time to topohere. (a) The thickness of the cellulose solution is controlled using a nylon mesh as a spacer. The mesh is wet with cellulose solution and placed between two hydrogels. (b) Adhesion energy as a function of time after contact for various thicknesses. (c) Time to adhere is quantified as the time for the adhesion energy to reach half of the equilibrium value. The time to adhere scales with the square of the thickness for both cellulose and chitosan topohesives.

required to achieve a gelation time of 10^{-4} s is then estimated by $h \sim (D_{\text{trigger}} t)^{1/2}$ to be ~30 nm. This thickness represents the lower limit of the scaling relation $t \sim h^2/D_{\text{trigger}}$, since if the adhesive solution is on the order of 30 nm thick, then the time scale for diffusion of stitch polymer into the adherends and the time scale for gelation of the stitch network are comparable. In that case, specific knowledge regarding the interplay of diffusion and gelation is required to predict whether sufficient topological entanglements will form.

In the above discussion, we have tacitly assumed that the kinetics of gelation is the same as that of adhesion. This picture is too simplistic, because adhesion energy depends on the amount of dissipation in a volume around the crack front. This dissipation can be affected by the polymers diffused into the adherends. For example, a calcium-crosslinked alginate network in topological entanglement with a polyacrylamide network greatly amplifies adhesion energy. To study this effect quantitatively would require a different experimental design, which would go beyond the scope of this paper. Furthermore, the effect of the nylon mesh is itself interesting, which may lead to an effect called "elastic dissipater" [43–45]. These and other aspects of topohesion will be studied in subsequent papers in this series.

4. Discussion of existing topohesives

The experimental findings here shed light onto existing topohesives, most of which have adhesion times on the order of hours. Alginate, poly(acrylic acid), and chitosan topohesives develop an adhesion energy of 50 J m^{-2} in approximately 10, 15, and 30 min and reach equilibrium in 60 min, 50 min, and 24 h, respectively [35–37]. These works may originate the misconception that topohesion is always slow. Additionally, this misconception of slowness may have been influenced by similar methods of adhesion for thermoplastics and elastomers.

Two thermoplastics can strongly adhere through physical entanglements of polymer chains diffused across the interface. Since the diffused polymer chains are not crosslinked, the adhesion is entirely due to interchain interactions resisting the pull out of polymer chains. The number of interchain interactions scales with the depth of interdiffusion, therefore requiring that the materials be placed in contact for a sufficiently long time to interdiffuse [46]. The materials must be annealed to promote interdiffusion, often for times on the order of hours [47]. For elastomers, this time is on the order of the relaxation time of the diffusing polymer, or $\sim 10^5$ s at 25 °C [48]. If sufficient interdiffusion does not occur, then adhesion is weak. By contrast, topological adhesion is due to intrachain bonding within the stitch network. Analogous to interlink bonds formed at the interface, intrachain bonding does not scale with the depth of diffusion, and therefore sufficient diffusion of stitch polymer beyond one mesh size is not required.

Two partially cured elastomers can strongly adhere by being brought into contact and allowed to finish curing. If the two materials polymerize by the same reaction mechanism, then adhesion will be due to chemical interlinking [49]. Adhesion between poly(dimethyl siloxane) (PDMS) elastomers is commonly achieved in this manner. As a recent example, adhesion was achieved by submerging a PDMS elastomer in a PDMS precursor solution and subsequently curing the solution [43]. By contrast, if one material is fully cured, or if the polymerization reactions are incompatible, then adhesion will be due to topological entanglement. For example, adhesion between two PDMS elastomers, one fully cured and one partially cured, can be achieved by bringing them into contact and finishing curing [50].

We next discuss the reported methods of topohesion of wet and elastic materials in terms of their gelation kinetics, and categorize them by the chemistry of the trigger. In all cases, we conclude that the rate-limiting step to adhere is the gelation of the stitching network. By identifying the variables that determine the time to gel, it is then possible to design the kinetics of gelation to tune the time to adhere.

We first consider topohesives triggered by a change in pH, including the cellulose topohesive studied in this paper. The first reported pH-triggered topohesive used chitosan as a stitch polymer (Fig. 5a) [35]. Chitosan is a pH-sensitive polymer with a pK_a of 6.5. Chitosan is an aqueous solution when pH < 6.5, and forms a network through hydrogen bonds when pH > 6.5 [51]. Additional pH-triggered topohesives have been developed using cellulose, alginate, and poly(4-amino-styrene) (PAS) [35]. The gelation kinetics are governed by the diffusion of hydronium and hydroxide ions. The adhesion time is thus a function of the diffusivity of the hydronium and hydroxide ions and the length scale for diffusion of these species. We showed in this paper that the adhesion time can be tuned by changing the thickness of the adhesive, with a scaling relation of $t \sim h^2$. It is possible that the addition of buffering species can delay the change in pH, and thus slow gelation.

Poly(acrylic acid) (PAA) can form an ionically crosslinked network through complexation of carboxylic acid groups on acrylic acid with iron (III) ions (Fig. 5b) [37]. Complexation has also been used to form an ionic alginate topohesive with calcium (II) ions [36]. The gelation kinetics are governed by the kinetics of ion association. The adhesion time is thus a function of the polymer and ion concentrations. Ion association is in general a fast reaction, and can lead to a brittle stitch network. To produce a stretchable stitch network with PAA, the authors delay gelation by adding citric acid [37]. Citric acid can bind to iron (III)

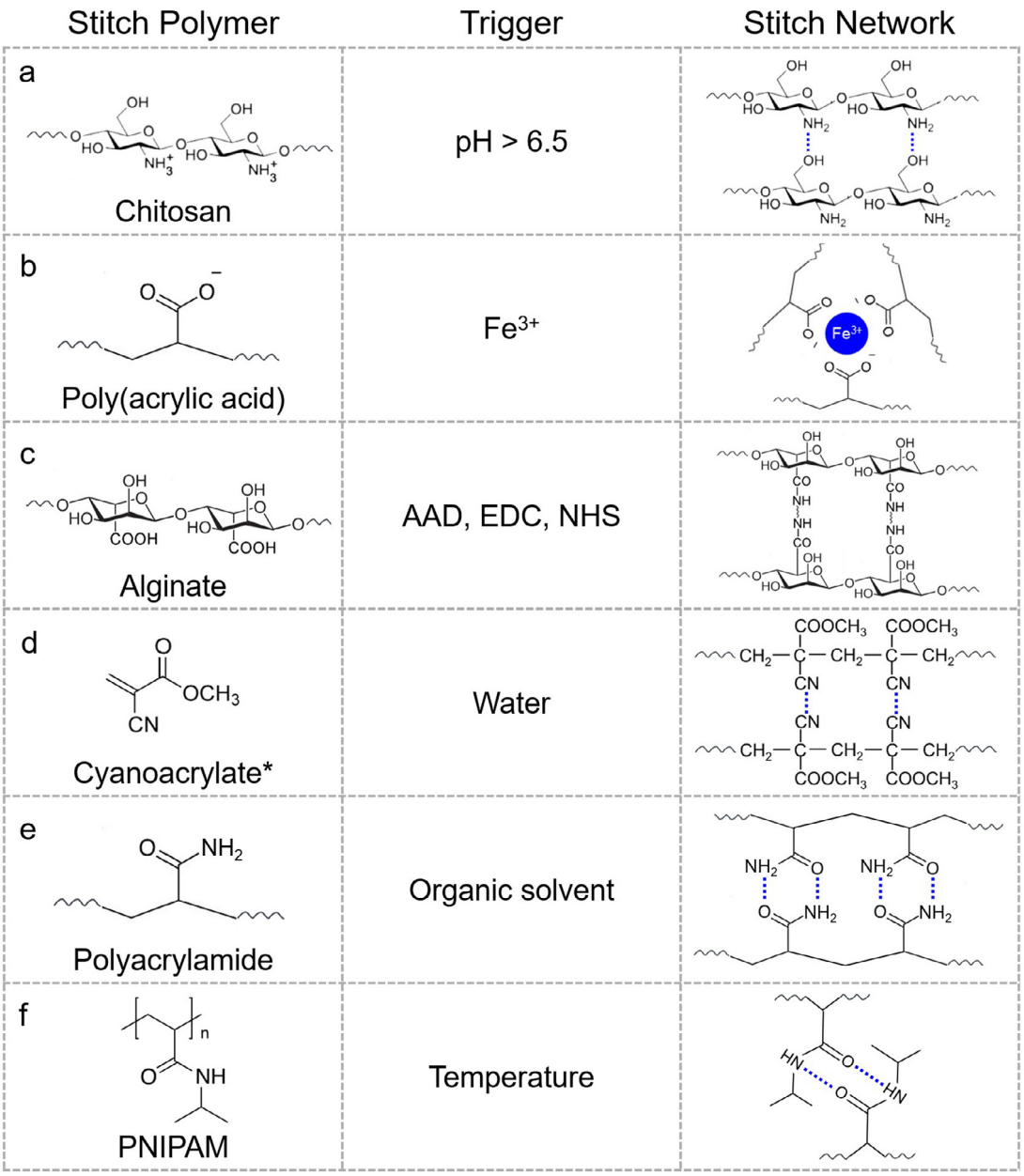

Fig. 5. Examples of topohesives for wet, elastic, strong adhesion. A trigger gelates the stitch polymer into the stitch network. Chitosan crosslinks into a noncovalent network by hydrogen bonds at pH > 6.5. Acrylic acid crosslinks into a noncovalent network by ionic bonding with iron (III) ions. Alginate crosslinks into a covalent network by chemical crosslinkers. Cyanoacrylate polymerizes in the presence of water and subsequently crosslinks into a noncovalent glassy network. It is possible that topohesives can be made using PAAm and PNIPAM stitch polymers triggered by exposure to an organic solvent and high temperature, respectively. *Cyanoacrylate monomers form stitch polymers.

in its conjugate base forms, and will debond when protonated. Therefore, adding citric acid lowers the concentration of iron (III) available for crosslinking PAA, delaying gelation until the pH changes. The authors optimize the concentrations to maximize the adhesion energy. The time at half max for the PAA topohesive is measured to be ∼10 min. We expect that the rate limiting step is the pH change of the solution, thus making the adhesion kinetics follow that of pH-triggered topohesives. In that case, the adhesion time is expected to scale with the square of the thickness.

Alginate is a biopolymer bearing carboxylic acid groups, which can form a covalent network through amide bonds triggered by adipic acid dihydrazide (AAD) and coupling agents 1-ethyl-3-(3-dimethylaminopropyl) (EDC) and N-hydroxysuccinimide (NHS) (Fig. 5c) [36,52]. The trigger for a covalent alginate topohesive is the chemical reaction between alginate, AAD, EDC, and NHS. The gelation kinetics are governed by the kinetics of the crosslinking reaction and the functionality of the alginate stitch polymer. The adhesion time is thus a function of the chemical rate constant and the reagent concentrations. The time at half max for an alginate topohesive is measured to be ∼15 min, where the rate limiting step is the chemical crosslinking reaction. Therefore, the adhesion time can be tuned by adjusting the reagent concentrations.

Cyanoacrylate is a monomer that polymerizes rapidly in contact with water (Fig. 5d). Subsequently, the polymer chains aggregate to form a glassy network through dense CN dipole–dipole interactions [38,53,54]. The trigger for cyanoacrylate is hydroxide ions found in water. The kinetics of gelation are governed by the kinetics of the polymerization reaction. The adhesion time is thus a function of the reaction rate constant for polymerization and the

reagent concentrations. In contrast to the previously mentioned topohesives, cyanoacrylate forms strong adhesion rapidly, on the order of seconds. This is achieved by having a large rate constant and using concentrated cyanoacrylate as the topohesive solution. The rate constant is reported as 1.9×10^9 M^{-1} s^{-1} at 25 °C [55]. However, due to rapid gelation, pure cyanoacrylate adhesives produce a dense and brittle stitch network. To achieve a transparent and stretchable stitch network, gelation can be delayed by diluting the monomer solution. This has been done by using organic solvents, producing tough adhesion with a less dense and stretchable stitch network [22]. The polycyanoacrylate may still form a glassy phase, but the interface is stretchable so long as the glassy phase takes the form of discrete particles, entangled with the adherend networks [38]. This method of adhesion is called molecular staples.

It is possible to envision topohesives using stimuli-responsive stitch polymers different from those previously reported. For example, PAAm is a hydrophilic polymer that forms a complex when placed in organic solvent (Fig. 5e). Therefore, an aqueous PAAm solution could be used to topohere two organogels, where the trigger is solvent exchange between water and the organic solvent. Since solvent exchange occurs due to diffusion, the kinetics of adhesion would be rate limited by the diffusion of solvent. As another example, poly(n-isopropylacrylamide) (PNIPAM) is a thermoresponsive polymer that is soluble in water at temperatures below 32 °C, and crosslinks into a polymer network at temperatures greater than 32 °C (Fig. 5f). Therefore, a PNIPAM solution at a lower temperature could be used to topohere two hydrogels at a higher temperature, where the trigger is the change in temperature. Since temperature changes due to thermal diffusion, the kinetics of adhesion would be rate limited by the diffusion of thermal energy. For both topohesives, the adhesion time could be tuned by varying the thickness of the topohesive solution.

A topohesive may be used to add functional groups to the surfaces of elastomers and hydrogels. Topohesion requires no functional groups from the adherends themselves. However, if the stitch network bears functional groups, then the surface of a material topologically entangled with the stitch network will also bear these functional groups. This method of functionalization is called topological prime, or topoprime for short. For elastomers, topoprime has been used to functionalize the surface of PDMS to be hydrophilic [56]. Additionally, functional groups for bonding can be added to the surface of PDMS, where adhesion to a hydrogel bearing functional groups can then be achieved by chemical interlinking [57]. Similarly, functional groups for bonding can be added to the surface of PAAm, where adhesion to an elastomer bearing functional groups can then be achieved by chemical interlinking [58]. If neither material has functional groups for interlinking, then stitch networks with compatible functional groups can be introduced to the surfaces of both materials separately. It is then possible to bond the two materials through chemical interlinking between the two superficial stitch networks. This has been used to achieve adhesion between preformed PDMS elastomers and PAAm hydrogels that initially have no functional groups for bonding [59]. The kinetics of topoprime will be governed by the kinetics of the topohesive used to form the superficial stitch network. In combination with 3D printing or microstamping, topohesives may create patterned functional groups on curved or flat surfaces. This approach may enable a broadly useful technology of topological lithography, or topolithography.

5. Conclusion

Strong topohesion can be superficial. The stitch network only needs to entangle with each adherend network by one polymer mesh size. Consequently, topohesion is rate-limited by gelation of the stitch network, not by diffusion of stitch polymers into the adherend networks. This picture dispels the misconceived myth that topohesion is always slow. We have demonstrated that topohesion can be rapid, and that the time to topohere is tunable. For pH-triggered topohesion, we propose that the time to adhere scales with the square of the thickness of topohesive. This scaling relation successfully predicts the time to adhere ranging from seconds to hours. The principle presented here enables the formulation of topohesives that accommodate a wide variety of applications and manufacturing processes, which often require particular properties, such as biocompatibility and on-demand detachment, as well as time to adhere, slow, rapid, and instant. For a given chemistry of topohesive, the gelation kinetics can be independently controlled. There is ample opportunity to formulate topohesives to enable unconventional applications. The world is full of networks, natural and synthetic, waiting to be stitched.

Experimental Section

Materials

All chemicals were purchased and used without further purification. Polyacrylamide hydrogels were formed from acrylamide monomer (AAm, Sigma Aldrich, A8887) with N,N'-Methylenebisacrylamide (MBAA, Sigma Aldrich, M7279) covalent crosslinker. Ammonium persulfate (APS, Sigma Aldrich, 248614) was used as the initiator for polymerization and N N' N'-Tetramethylethylenediamine (TEMED, Sigma Aldrich, T7024) was used as the crosslinking accelerator. Cellulose powder (Sigma Aldrich, 435236), urea powder (Sigma Aldrich, U5128), and sodium hydroxide pellets (Macron) were used to create the cellulose topohesive solution. Nylon meshes were purchased and used without further modification, including measured thicknesses of 50 (McMaster Carr, 9318T25), 120 (McMaster Carr, 9318T23), and 180 μm (McMaster Carr, 9318T45).

Preparation of Hydrogels

Polyacrylamide hydrogels were formed from a 2 M acrylamide solution, produced by dissolving 40.56 g acrylamide powder into 300 mL deionized water. MBAA and TEMED were mixed with acrylamide solution at weight ratios of reactant to acrylamide of 0.0006:1 and 0.0028:1, respectively. This solution was then mixed with APS with an APS to acrylamide weight ratio of 0.01:1 and poured into glass molds. The molds were covered with a glass plate and stored at ambient conditions until polymerization was complete. The hydrogel had final dimensions of 5 cm long, 2 cm wide, and 3 mm thick.

Procedure of bonding

The cellulose topohesive was produced following the procedure of Cai and Zhang [42]. Briefly, an aqueous solution was produced with 7 wt% urea and 12 wt% sodium hydroxide. After the solution was cooled to −20 °C, cellulose powder was added to the desired cellulose polymer concentration, either 0.5, 1, 1.5, or 2 wt%. This solution was then stirred vigorously at room temperature until all cellulose powder was dissolved. The prepared cellulose solution was applied to the surface of one hydrogel and spread until the surface was uniformly wetted. Another hydrogel was placed on top and compressed to approximately ∼5% strain to squeeze out excess solution. Compression was then removed and the sample was left in a plastic bag until testing to prevent dehydration.

Adhesion with controlled thickness of cellulose solution was achieved using nylon meshes of varying thickness. The nylon

mesh was dipped into the prepared cellulose solution, removed, and wiped multiple times on a glass slide to remove excess solution. Once preparation was complete, the cellulose solution was only contained within the pores of the mesh. The wetted mesh was applied to the surface of one hydrogel, and another hydrogel was then immediately placed on top. Compression was only applied to ensure wetted contact between the gels and the mesh. Since the adhesion developed rapidly in these experiments, the sample was tested immediately after contact was made. The nylon mesh was not removed between contact and testing.

180-degree peeling tests for measuring adhesion energy

Samples were tested using an Instron tensile testing machine (Series 5900) with a 100 N load cell. All tests were conducted at room temperature and in open air. The back sides of the hydrogels were glued to an inextensible and flexible 100-μm-thick polyester film (clear polyester film, McMaster-Carr) using cyanoacrylate glue (Krazy glue). The free ends of the backing layer were glued to pieces of acrylic sheet and then clamped in the grips of the tensile tester. The ends were peeled at a rate of 0.4 mm s^{-1} for all tests and the force was measured as a function of displacement. The measured force increases initially, and then reaches a plateau value at steady state. The adhesion energy is calculated as twice the steady state peel force divided by the width of the sample. For measuring adhesion energy as a function of time, the two hydrogels were loaded into the tensile tester separately, bonded, and then tested immediately.

Declaration of competing interest

The authors declare that they have no known competing financial interests or personal relationships that could have appeared to influence the work reported in this paper.

Acknowledgments

This work was supported by MRSEC (DMR-14-20570). J. Kim acknowledges financial support from the Kwanjeong Educational Foundation.

References

[1] O. Wichterle, D. Lím, Hydrophilic gels for biological use, Nature 185 (1960) 117–118, http://dx.doi.org/10.1038/185117a0.
[2] H. Fan, J.P. Gong, Fabrication of bioinspired hydrogels: Challenges and opportunities, Macromolecules (2020) acs.macromol.0c00238, http://dx.doi.org/10.1021/acs.macromol.0c00238.
[3] N. Annabi, Y.-N. Zhang, A. Assmann, E.S. Sani, G. Cheng, A.D. Lassaletta, A. Vegh, B. Dehghani, G.U. Ruiz-Esparza, X. Wang, S. Gangadharan, A.S. Weiss, A. Khademhosseini, Engineering a highly elastic human protein–based sealant for surgical applications, Sci. Transl. Med. 9 (2017) eaai7466, http://dx.doi.org/10.1126/scitranslmed.aai7466.
[4] N. Lang, M.J. Pereira, Y. Lee, I. Friehs, N.V. Vasilyev, E.N. Feins, K. Ablasser, E.D. O'Cearbhaill, C. Xu, A. Fabozzo, R. Padera, S. Wasserman, F. Freudenthal, L.S. Ferreira, R. Langer, J.M. Karp, P.J. del Nido, A blood-resistant surgical glue for minimally invasive repair of vessels and heart defects, Sci. Transl. Med. 6 (2014) 218ra6, http://dx.doi.org/10.1126/scitranslmed.3006557.
[5] J. Li, A.D. Celiz, J. Yang, Q. Yang, I. Wamala, W. Whyte, B.R. Seo, N.V. Vasilyev, J.J. Vlassak, Z. Suo, D.J. Mooney, Tough adhesives for diverse wet surfaces, Science 357 (2017) 378–381, http://dx.doi.org/10.1126/science.aah6362.
[6] E. Shirzaei Sani, A. Kheirkhah, D. Rana, Z. Sun, W. Foulsham, A. Sheikhi, A. Khademhosseini, R. Dana, N. Annabi, Sutureless repair of corneal injuries using naturally derived bioadhesive hydrogels, Sci. Adv. 5 (2019) eaav1281, http://dx.doi.org/10.1126/sciadv.aav1281.
[7] B. Sharma, S. Fermanian, M. Gibson, S. Unterman, D.A. Herzka, B. Cascio, J. Coburn, A.Y. Hui, N. Marcus, G.E. Gold, J.H. Elisseeff, Human cartilage repair with a photoreactive adhesive-hydrogel composite, Sci. Transl. Med. 5 (2013) 167ra6, http://dx.doi.org/10.1126/scitranslmed.3004838.
[8] N. Annabi, K. Yue, A. Tamayol, A. Khademhosseini, Elastic sealants for surgical applications, Eur. J. Pharm. Biopharm. 95 (2015) 27–39, http://dx.doi.org/10.1016/j.ejpb.2015.05.022.
[9] S.O. Blacklow, J. Li, B.R. Freedman, M. Zeidi, C. Chen, D.J. Mooney, Bioinspired mechanically active adhesive dressings to accelerate wound closure, Sci. Adv. 5 (2019) eaaw3963, http://dx.doi.org/10.1126/sciadv.aaw3963.
[10] P.J.M. Bouten, M. Zonjee, J. Bender, S.T.K. Yauw, H. van Goor, J.C.M. van Hest, R. Hoogenboom, The chemistry of tissue adhesive materials, Prog. Polym. Sci. 39 (2014) 1375–1405, http://dx.doi.org/10.1016/j.progpolymsci.2014.02.001.
[11] M.W. Grinstaff, Designing hydrogel adhesives for corneal wound repair, Biomaterials 28 (2007) 5205–5214, http://dx.doi.org/10.1016/j.biomaterials.2007.08.041.
[12] T.R. Hoare, D.S. Kohane, Hydrogels in drug delivery: Progress and challenges, Polymer 49 (2008) 1993–2007, http://dx.doi.org/10.1016/j.polymer.2008.01.027.
[13] V.V. Khutoryanskiy, Advances in mucoadhesion and mucoadhesive polymers, Macromol. Biosci. 11 (2011) 748–764, http://dx.doi.org/10.1002/mabi.201000388.
[14] J. Li, D.J. Mooney, Designing hydrogels for controlled drug delivery, Nat. Rev. Matter. 1 (2016) 16071, http://dx.doi.org/10.1038/natrevmats.2016.71.
[15] M.R. Prausnitz, R. Langer, Transdermal drug delivery, Nat. Biotechnol. 26 (2008) 1261–1268, http://dx.doi.org/10.1038/nbt.1504.
[16] S. Baik, H.J. Lee, D.W. Kim, J.W. Kim, Y. Lee, C. Pang, Bioinspired adhesive architectures: From skin patch to integrated bioelectronics, Adv. Matter. 31 (2019) 1803309, http://dx.doi.org/10.1002/adma.201803309.
[17] Y. Liu, J. Liu, S. Chen, T. Lei, Y. Kim, S. Niu, H. Wang, X. Wang, A.M. Foudeh, J.B.-H. Tok, Z. Bao, Soft and elastic hydrogel-based microelectronics for localized low-voltage neuromodulation, Nat. Biomed. Eng. 3 (2019) 58–68, http://dx.doi.org/10.1038/s41551-018-0335-6.
[18] H. Sheng, X. Wang, N. Kong, W. Xi, H. Yang, X. Wu, K. Wu, C. Li, J. Hu, J. Tang, J. Zhou, S. Duan, H. Wang, Z. Suo, Neural interfaces by hydrogels, Extreme Mech. Lett. 30 (2019) 100510, http://dx.doi.org/10.1016/j.eml.2019.100510.
[19] H. Yuk, B. Lu, X. Zhao, Hydrogel bioelectronics, Chem. Soc. Rev. (2018) http://dx.doi.org/10.1039/C8CS00595H.
[20] H.-R. Lee, C.-C. Kim, J.-Y. Sun, Stretchable ionics – A promising candidate for upcoming wearable devices, Adv. Matter. 30 (2018) 1704403, http://dx.doi.org/10.1002/adma.201704403.
[21] J.Y. Sun, C. Keplinger, G.M. Whitesides, Z. Suo, Ionic skin, Adv. Matter. 26 (2014) 7608–7614, http://dx.doi.org/10.1002/adma.201403441.
[22] D. Wirthl, R. Pichler, M. Drack, G. Kettlguber, R. Moser, R. Gerstmayr, F. Hartmann, E. Bradt, R. Kaltseis, C.M. Siket, S.E. Schausberger, S. Hild, S. Bauer, M. Kaltenbrunner, Instant tough bonding of hydrogels for soft machines and electronics, Sci. Adv. 3 (2017) e1700053, http://dx.doi.org/10.1126/sciadv.1700053.
[23] C. Yang, Z. Suo, Hydrogel ionotronics, Nat. Rev. Matter. 3 (2018) 125–142, http://dx.doi.org/10.1038/s41578-018-0018-7.
[24] H. Yang, C. Li, M. Yang, Y. Pan, Q. Yin, J. Tang, H.J. Qi, Z. Suo, Printing hydrogels and elastomers in arbitrary sequence with strong adhesion, Adv. Funct. Mater. 29 (2019) 1901721, http://dx.doi.org/10.1002/adfm.201901721.
[25] A. Chortos, J. Liu, Z. Bao, Pursuing prosthetic electronic skin, Nature Mater. 15 (2016) 937–950, http://dx.doi.org/10.1038/nmat4671.
[26] T.R. Ray, J. Choi, A.J. Bandodkar, S. Krishnan, P. Gutruf, L. Tian, R. Ghaffari, J.A. Rogers, Bio-integrated wearable systems: A comprehensive review, Chem. Rev. 119 (2019) 5461–5533, http://dx.doi.org/10.1021/acs.chemrev.8b00573.
[27] D.J. Lipomi, M. Vosgueritchian, B.C.-K. Tee, S.L. Hellstrom, J.A. Lee, C.H. Fox, Z. Bao, Skin-like pressure and strain sensors based on transparent elastic films of carbon nanotubes, Nat. Nanotechnol. 6 (2011) 788–792, http://dx.doi.org/10.1038/nnano.2011.184.
[28] T. Shay, O.D. Velev, M.D. Dickey, Soft electrodes combining hydrogel and liquid metal, Soft Matter. 14 (2018) 3296–3303, http://dx.doi.org/10.1039/C8SM00337H.
[29] J. Yang, R. Bai, B. Chen, Z. Suo, Hydrogel adhesion: A supramolecular synergy of chemistry, topology, and mechanics, Adv. Funct. Matter. 30 (2019) 1901693, http://dx.doi.org/10.1002/adfm.201901693.
[30] S. Rose, A. Prevoteau, P. Elzière, D. Hourdet, A. Marcellan, L. Leibler, Nanoparticle solutions as adhesives for gels and biological tissues, Nature 505 (2014) 382–385, http://dx.doi.org/10.1038/nature12806.
[31] Q. Liu, G. Nian, C. Yang, S. Qu, Z. Suo, Bonding dissimilar polymer networks in various manufacturing processes, Nature Commun. 9 (2018) 846, http://dx.doi.org/10.1038/s41467-018-03269-x.
[32] C.K. Roy, H.L. Guo, T.L. Sun, A.B. Ihsan, T. Kurokawa, M. Takahata, T. Nonoyama, T. Nakajima, J.P. Gong, Self-adjustable adhesion of polyampholyte hydrogels, Adv. Matter. 27 (2015) 7344–7348, http://dx.doi.org/10.1002/adma.201504059.
[33] Y. Wang, K. Jia, C. Xiang, J. Yang, X. Yao, Z. Suo, Instant, tough, noncovalent adhesion, ACS Appl. Matter. Interfaces 11 (2019) 40749–40757, http://dx.doi.org/10.1021/acsami.9b10995.
[34] H. Yuk, C.E. Varela, C.S. Nabzdyk, X. Mao, R.F. Padera, E.T. Roche, X. Zhao, Dry double-sided tape for adhesion of wet tissues and devices, Nature 575 (2019) 169–174, http://dx.doi.org/10.1038/s41586-019-1710-5.

[35] J. Yang, R. Bai, Z. Suo, Topological adhesion of wet materials, Adv. Matter. 30 (2018) 1800671, http://dx.doi.org/10.1002/adma.201800671.
[36] J. Steck, J. Yang, Z. Suo, Covalent topological adhesion, ACS Macro Lett. 8 (2019) 754–758, http://dx.doi.org/10.1021/acsmacrolett.9b00325.
[37] Y. Gao, K. Wu, Z. Suo, Photodetachable adhesion, Adv. Matter. 31 (2018) 1806948, http://dx.doi.org/10.1002/adma.201806948.
[38] B. Chen, J. Yang, R. Bai, Z. Suo, Molecular staples for tough and stretchable adhesion in integrated soft materials, Adv. Healthc. Matter. 8 (2019) 1900810, http://dx.doi.org/10.1002/adhm.201900810.
[39] H. Yang, C. Li, J. Tang, Z. Suo, Strong and degradable adhesion of hydrogels, ACS Appl. Bio Matter. 2 (2019) 1781–1786, http://dx.doi.org/10.1021/acsabm.9b00103.
[40] D. Klemm, B. Heublein, H.-P. Fink, A. Bohn, Cellulose: Fascinating biopolymer and sustainable raw material, Angew. Chem. Int. Ed. 44 (2005) 3358–3393, http://dx.doi.org/10.1002/anie.200460587.
[41] B.L. Peng, N. Dhar, H.L. Liu, K.C. Tam, Chemistry and applications of nanocrystalline cellulose and its derivatives: A nanotechnology perspective, Can. J. Chem. Eng. 89 (2011) 1191–1206, http://dx.doi.org/10.1002/cjce.20554.
[42] J. Cai, L. Zhang, Rapid dissolution of cellulose in LiOH/urea and NaOH/urea aqueous solutions, Macromol. Biosci. 5 (2005) 539–548, http://dx.doi.org/10.1002/mabi.200400222.
[43] Z. Wang, C. Xiang, X. Yao, P. Le Floch, J. Mendez, Z. Suo, Stretchable materials of high toughness and low hysteresis, Proc. Natl. Acad. Sci. 116 (2019) 5967–5972, http://dx.doi.org/10.1073/pnas.1821420116.
[44] C. Xiang, Z. Wang, C. Yang, X. Yao, Y. Wang, Z. Suo, Stretchable and fatigue-resistant materials, Matter. Today (2019) S1369702119307606, http://dx.doi.org/10.1016/j.mattod.2019.08.009.
[45] J. Liu, C. Yang, T. Yin, Z. Wang, S. Qu, Z. Suo, Polyacrylamide hydrogels. II. elastic dissipater, J. Mech. Phys. Solids 133 (2019) 103737, http://dx.doi.org/10.1016/j.jmps.2019.103737.
[46] E. Raphael, P.G. De Gennes, Rubber-rubber adhesion with connector molecules, J. Phys. Chem. 96 (1992) 4002–4007, http://dx.doi.org/10.1021/j100189a018.
[47] C. Creton, H.R. Brown, K.R. Shull, Molecular weight effects in chain pullout, Macromolecules 27 (1994) 3174–3183, http://dx.doi.org/10.1021/ma00090a010.
[48] M.D. Ellul, A.N. Gent, The role of molecular diffusion in the adhesion of elastomers, J. Polym. Sci. Polym. Phys. Ed. 22 (1984) 1953–1968, http://dx.doi.org/10.1002/pol.1984.180221108.
[49] R.-J. Chang, A.N. Gent, Effect of interfacial bonding on the strength of adhesion of elastomers. I. Self-adhesion, J. Polym. Sci. Polym. Phys. Ed. 19 (1981) 1619–1633, http://dx.doi.org/10.1002/pol.1981.180191011.
[50] A.N. Gent, R.H. Tobias, Effect of interfacial bonding on the strength of adhesion of elastomers. III. Interlinking by molecular entanglements, J. Polym. Sci. Polym. Phys. Ed. 22 (1984) 1483–1490, http://dx.doi.org/10.1002/pol.1984.180220812.
[51] S. Ladet, L. David, A. Domard, Multi-membrane hydrogels, Nature 452 (2008) 76–79, http://dx.doi.org/10.1038/nature06619.
[52] X. Zhao, N. Huebsch, D.J. Mooney, Z. Suo, Stress-relaxation behavior in gels with ionic and covalent crosslinks, J. Appl. Phys. 107 (2010) 063509, http://dx.doi.org/10.1063/1.3343265.
[53] G. Henrici-Olivé, S. Olivé, Molecular interactions and macroscopic properties of polyacrylonitrile and model substances, in: Chemistry, Springer Berlin Heidelberg, Berlin, Heidelberg, 1979, pp. 123–152, http://dx.doi.org/10.1007/3-540-09442-3_6.
[54] K.L. Shantha, S. Thennarasu, N. Krishnamurti, Developments and applications of cyanoacrylate adhesives, J. Adhes. Sci. Technol. 3 (1989) 237–260, http://dx.doi.org/10.1163/156856189X00191.
[55] W.M. Meylan, P.H. Howard, Computer estimation of the atmospheric gas-phase reaction rate of organic compounds with hydroxyl radicals and ozone, Chemosphere 26 (1993) 2293–2299, http://dx.doi.org/10.1016/0045-6535(93)90355-9.
[56] X. Yang, C. Yang, J. Liu, X. Yao, Z. Suo, Topological prime, Sci. China Technol. Sci. (2020) http://dx.doi.org/10.1007/s11431-019-1498-y.
[57] S. Cheng, Y.S. Narang, C. Yang, Z. Suo, R.D. Howe, Stick-on large-strain sensors for soft robots, Adv. Matter. Interfaces 6 (2019) 1900985, http://dx.doi.org/10.1002/admi.201900985.
[58] J. Yang, R. Bai, J. Li, C. Yang, X. Yao, Q. Liu, J.J. Vlassak, D.J. Mooney, Z. Suo, Design molecular topology for wet–dry adhesion, ACS Appl. Matter. Interfaces 11 (2019) 24802–24811, http://dx.doi.org/10.1021/acsami.9b07522.
[59] S. Cheng, C. Yang, X. Yang, Z. Suo, Dual-primer adhesion for polymer networks of dissimilar chemistries, Rev. (n.d.).